System-Level Performance Analysis of LoRa-Based LEO Satellite Constellations for IoT Communications

Quantao Yu, Deepak Mishra, *Senior Member, IEEE*, Hua Wang, *Member, IEEE*, Dongxuan He, *Member, IEEE*, Jinhong Yuan, *Fellow, IEEE*, and Michail Matthaiou, *Fellow, IEEE*

***Abstract*—In this letter, we propose a novel spherical stochastic geometry (SG)-based analytical framework for characterizing the system-level performance of Long-Range (LoRa)-based low Earth orbit (LEO) satellite constellations. Specifically, the LEO satellite constellations and the terrestrial LoRa end-devices (EDs) are modeled by a Binomial point process (BPP) and Poisson point process (PPP), respectively. Tractable analytical expressions are derived for the uplink coverage probability and area spectral efficiency, where the trends of both performance metrics are unveiled with respect to the EDs' density and the spreading factor (SF). In particular, the uplink coverage probability and the area spectral efficiency is proven to be a monotonically decreasing function and a unimodal function of the EDs' density, respectively. Numerical simulations not only verify our theoretical analysis but also provide some useful insights into the practical design and implementation of LoRa-based LEO satellite constellations for Internet of Things (IoT) communications.**

***Index Terms*—Internet of Things (IoT), Long-Range (LoRa), low Earth orbit (LEO) satellite constellations, performance analysis, stochastic geometry (SG).**

I. Introduction

OVER the past few years, Long-Range (LoRa) has attracted widespread attention from both academia and industry due to its superior capabilities to provide energy-efficient and cost-effective communications for various Internet of Things (IoT) applications [1]. Moreover, with the emerging innovation of launch and propulsion technologies, as well as the rapid development of miniaturized satellites known as CubeSats [2], exploiting low Earth orbit (LEO) satellite constellations has become an efficient means to provide ubiquitous IoT connectivity [3]. In this context, an accurate system-level performance analysis of LoRa-based LEO satellite constellations is of great importance for the practical design and implementation of such a new paradigm.

To address this issue, the authors in [4] analyzed the uplink performance of LoRa-based LEO satellite IoT systems. However, the system model in [4] only considered a single LEO satellite while the performance analysis focused on the link-level rather than system-level. In [5], the authors investigated the uplink performance of IoT-over-satellite networks in terms of coverage probability and normalized throughput based on LEO satellite constellations. Moreover, the authors in [6] proposed a stochastic geometry (SG)-based analytical framework for characterizing the coverage performance of IoT-over-satellite networks in both direct access and indirect access scenarios, where the IoT end-devices (EDs) and LEO satellite constellations were modeled by a Poisson cluster process (PCP) and Binomial point process (BPP), respectively. However, the system models proposed in [5], [6] did not take into account the unique features of LoRa networks, including the chirp spread spectrum (CSS) modulation used in physical (PHY) layer and the duty cycle-limited random access employed in medium access control (MAC) layer, which however play a dominant role in determining the overall performance of LoRa-based LEO satellite constellations. To the best of our knowledge, an accurate system-level performance analysis of such a new paradigm has not been well investigated in the existing literature.

In this letter, we focus on the system-level performance analysis of LoRa-based LEO satellite constellations to fill this gap, where the main contributions are summarized as follows:

1) A novel analytical framework for characterizing the system-level performance of LoRa-based LEO satellite constellations is proposed based on spherical SG, where both the channel characteristics of satellite communications and the unique features of LoRa networks are considered in our proposed system model.
2) Tractable analytical expressions for the uplink coverage probability and area spectral efficiency are derived under the BPP constellation model and Poisson point process (PPP) EDs model, where the trends of both performance metrics are unveiled with respect to the EDs' density and the spreading factor (SF). In particular, the uplink coverage probability and the area spectral efficiency is proven to be a monotonically decreasing function and a unimodal function of the EDs' density, respectively.

Notations: Throughout this paper, we denote $F_X(x)$ and

This work was supported in part by the National Key Research and Development Program of China under Grant 2024YFE0200404; in part by the National Key Research and Development Program of China under Grant 2020YFB1807900; in part by the China Scholarship Council (CSC); and in part by the U.K. Engineering and Physical Sciences Research Council (EPSRC) (grant No. EP/X04047X/1). This work was partially funded by the Australian Research Council (ARC) Discovery Early Career Researcher Award (DECRA) - DE230101391. The work of M. Matthaiou has received funding from the European Research Council (ERC) under the European Union's Horizon 2020 research and innovation programme (grant agreement No. 101001331). *(Corresponding authors: Hua Wang; Dongxuan He.)*

Quantao Yu, Hua Wang, and Dongxuan He are with the School of Information and Electronics, Beijing Institute of Technology, Beijing 100081, China (e-mails: 3120215432@bit.edu.cn; wanghua@bit.edu.cn; dongxuan_he@bit.edu.cn).

Deepak Mishra and Jinhong Yuan are with the School of Electrical Engineering and Telecommunications, University of New South Wales Sydney, NSW 2052, Australia (e-mails: d.mishra@unsw.edu.au; j.yuan@unsw.edu.au).

Michail Matthaiou is with the Centre for Wireless Innovation (CWI), Queen's University Belfast, BT3 9DT Belfast, U.K. (e-mail: m.matthaiou@qub.ac.uk).

$f_X(x)$ as the cumulative distribution function (CDF) and the probability density function (PDF) of a random variable X; $\max\{\cdot\}$, $\lceil\cdot\rceil$, $\exp(\cdot)$, and $\ln(\cdot)$ are the maximum, ceiling, natural exponential, and natural logarithm operations; $\mathbb{E}[\cdot]$ and $\Pr\{\cdot\}$ denote the mathematical expectation and probability measure, respectively.

II. System Model

A. Network Model

1) Constellation model: Let us denote R as the radius of Earth. For the constellation model, we assume that there are N_s LEO satellites randomly distributed at the same orbit altitude H, while the satellite locations are characterized by a homogeneous spherically wrapped BPP Φ_s. Note that the commonly used constellation models in practice are based on Walker-Star and/or Walker-Delta constellations, in which the distribution of satellites is deterministic and correlated. However, such deterministic constellations require complex mathematical modeling, whereas random constellations modeled by BPPs facilitate a tractable analytical performance analysis of LEO satellite networks. Moreover, it has been substantiated that the BPP constellation model provides a lower bound on the system-level coverage performance, which behaves closely to the deterministic constellations modeled by Walker-Star and/or Walker-Delta [5].

2) EDs model: The LoRa EDs are assumed to be uniformly distributed within the satellite footprint, whereas the distribution of the LoRa EDs is modeled by a PPP Φ with intensity λ (i.e., the density of LoRa EDs). Moreover, since different spreading factors (SFs), ranging from 7 to 12, are adopted in LoRa networks, we consider that there are $\mathcal{K}$ classes of LoRa EDs (i.e., $\mathcal{K}=6$) and that each class of LoRa EDs is assigned a SF and modeled by an independent PPP Φ_k with intensity λ_k, where $k\in\{7,...,12\}$ denotes the SF. As a next step, it is convenient to investigate the specific performance for any class of LoRa EDs (i.e., the impact of SF on the system performance). For simplicity, a random SF allocation scheme is adopted in this paper, where each ED is randomly assigned a SF and the proportion that an ED is assigned the SF k is $\rho_k=\frac{1}{\mathcal{K}},\forall k$.[1] Therefore, the density of EDs of class k is given by $\lambda_k=\rho_k\lambda$.

All classes of LoRa EDs are equipped with an omnidirectional antenna with the same effective isotropic radiated power (EIRP) P_t. In addition, we denote Φ_k^A as the PPP of active LoRa EDs of class k with intensity $p_k\lambda_k$, where $p_k=\frac{T_k}{T_p}$ is the active probability with T_k and T_p representing the Time on Air (ToA) of class k and the average packet inter-arrival time, respectively. Specifically, the ToA of class k is given by [7]

$$T_k=\frac{2^k}{B}\left(N_p+12.25+\max\left\{\left\lceil\frac{8L-4k+28+16C-20E}{4k}\right\rceil(C_r+4),0\right\}\right), \tag{1}$$

[1]More efficient SF allocation schemes can be further investigated for the performance optimization of LoRa-based LEO satellite constellations, which is an interesting topic left for future research.

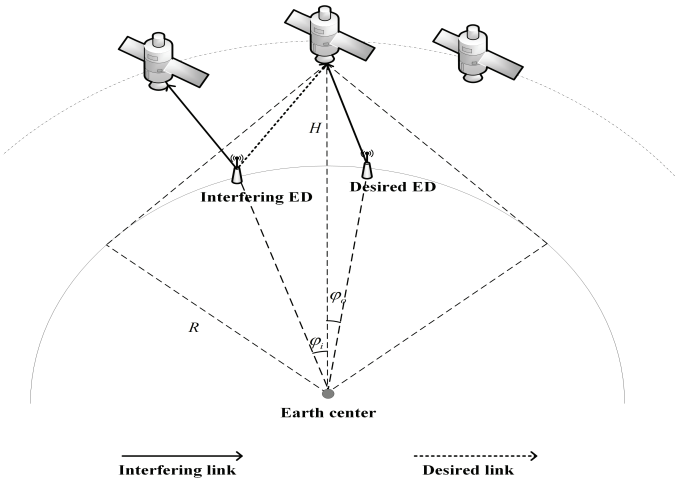

Fig. 1. An illustration of the network model for LoRa-based LEO satellite constellations.

where B is the configured bandwidth, N_p is the number of preamble symbols, L denotes the PHY payload length in bytes, C_r is the code rate, C is the cyclic redundancy check (CRC) indicator, and E is the PHY layer header indicator.

3) Geometric model: As depicted in Fig. 1, we assume that each LoRa ED associates with its nearest satellite. To simplify the mathematical representation, we use the contact angle φ to denote the relative location between a LoRa ED and its serving satellite, i.e., the Earth-centered zenith angle, while the maximum contact angle φ_m is given as [8]

$$\varphi_m=\cos^{-1}\left(\frac{R}{R+H}\right). \tag{2}$$

According to the characteristics of the BPP constellation model, the PDF of the contact angle is given by [8]

$$f_\varphi(x)=\frac{N_s}{2}\sin x\exp\left[-\frac{N_s}{2}(1-\cos x)\right],\ x\geq 0. \tag{3}$$

Moreover, given the contact angle φ, the distance between a LoRa ED and a LEO satellite can be obtained using the basic cosine theorem as [9]

$$d(\varphi)=\sqrt{(R+H)^2+R^2-2R(R+H)\cos\varphi}. \tag{4}$$

B. Channel Model

1) Large-scale fading: For the sake of simplicity, the free space path-loss model is adopted to characterize the large-scale fading, which is suitable for the Internet of remote things, where the LoRa EDs are typically deployed in open remote areas. Specifically, it is given as

$$L(d(\varphi))=\left(\frac{c}{4\pi f_c d(\varphi)}\right)^2, \tag{5}$$

where c is the speed of light and f_c is the carrier frequency. Notably, once the additional path-loss, like atmospheric loss and pointing loss, is included in the channel model, the link budget of our considered system may become insufficient and thus a safety link margin should be added in practice. Nevertheless, it is worth noting that these additional path-losses can be easily incorporated into our channel model by

adding the corresponding path-loss factors into the large-scale fading.

2) Small-scale fading: In addition, the small-scale fading of the desired and interfering LoRa EDs of class k, i.e., $h_{o,k}$ and $h_{i,k}$, follows an independent and identically distributed (i.i.d.) shadowed Rician (SR) fading with Nakagami fading coefficient m, the half average power of scattered component b_0 and the average power of line-of-sight component Ω. The CDF and PDF of the SR channel gain $|h|^2$ are given by [9]

$$F_{|h|^2}(x) = \left(\frac{2b_0m}{2b_0m+\Omega}\right)^m \sum_{z=0}^{\infty} \frac{(m)_z}{z!\Gamma(z+1)} \left(\frac{\Omega}{2b_0m+\Omega}\right)^z \times \gamma\left(z+1, \frac{1}{2b_0}x\right), \tag{6}$$

$$f_{|h|^2}(x) = \left(\frac{2b_0m}{2b_0m+\Omega}\right)^m \frac{1}{2b_0} \exp\left(-\frac{x}{2b_0}\right) \times {}_1F_1\left(m, 1, \frac{\Omega x}{2b_0(2b_0m+\Omega)}\right), \tag{7}$$

respectively, where $\Gamma(\cdot)$ denotes the Gamma function, $\gamma(\cdot,\cdot)$ is the lower incomplete Gamma function, $(\cdot)_z$ is the Pochhammer symbol, while ${}_1F_1(\cdot,\cdot,\cdot)$ is the confluent hypergeometric function. Since (6) and (7) are too complex to calculate, we approximate the SR channel gain $|h|^2$ by a Gamma random variable with its CDF and PDF denoted as [10]

$$F_{|h|^2}(x) \approx \frac{1}{\Gamma(\alpha)}\gamma\left(\alpha, \frac{x}{\beta}\right), \ x \geq 0, \tag{8}$$

$$f_{|h|^2}(x) \approx \frac{1}{\beta^\alpha\Gamma(\alpha)}x^{\alpha-1}\exp\left(-\frac{x}{\beta}\right), \ x \geq 0, \tag{9}$$

where $\alpha \triangleq \frac{m(2b_0+\Omega)^2}{4mb_0^2+4mb_0\Omega+\Omega^2}$ and $\beta \triangleq \frac{4mb_0^2+4mb_0\Omega+\Omega^2}{m(2b_0+\Omega)}$ denote the shape and scale parameters, respectively.

C. Signal Model

As depicted in Fig. 1, we consider the aggregated inter-ED interference at one of the serving satellites. For our considered LoRa-based LEO satellite constellations, inter-ED interference consists of the same SF (co-SF) interference and the different SF (inter-SF) interference. It has been shown in [11] that interfering EDs with different SFs have an average rejection signal-to-interference (SIR) threshold of -16 dB. Therefore, different SFs can be considered to be quasi-orthogonal [7] and only the impact of dominant co-SF interference is considered in the signal model. Moreover, we denote $\kappa \in [0,1]$ as the interference mitigation factor, which captures the impact of random access on the overall system performance. Accordingly, let us denote $s_{o,k}$ and $s_{i,k}$ as the unit-power transmitted signal from the desired and interfering LoRa EDs of class k, respectively, while the received signal of class k can be expressed as

$$r_k = \underbrace{\sqrt{P_tGL\left(d\left(\varphi_{o,k}\right)\right)}h_{o,k}s_{o,k}}_{\text{desired signal}} + \underbrace{w_k}_{\text{noise}} + \underbrace{\kappa \sum_{i\in\Phi_k^A\setminus o} \sqrt{P_tGL\left(d\left(\varphi_{i,k}\right)\right)}h_{i,k}s_{i,k}}_{\text{interfering signal}}, \tag{10}$$

where G represents the satellite antenna gain, $w_k \sim \mathcal{CN}\left(0,\sigma^2\right)$ denotes the complex circularly symmetric additive white Gaussian noise (AWGN). Note that $\sigma^2 = -174 + N_F + 10\log_{10}B$ with N_F representing the receiver's noise figure. We point out that the Doppler effect is not taken into account in the signal model for simplicity since both laboratory and flight testings have verified the strong immunity of LoRa-based LEO satellite communications to it [12].

III. Performance Analysis

A. Conditional Access Probability Analysis

Given the waveform properties of CSS modulation employed in LoRa PHY layer, the impact of noise and co-SF interference on the received signal demodulation should be separately considered [13]. On one hand, by availing of the processing gain of CSS modulation, the received signal can be demodulated even when the received SNR is negative. On the other hand, however, the SIR demodulation threshold should be at least larger than 0 dB for a successful demodulation while the empirical SIR demodulation threshold value is 6 dB in LoRa networks [7], [13]. Therefore, for a typical LoRa network, the successful transmission occurs only if both the SNR and SIR of the received signal exceed their corresponding thresholds. Hence, the conditional access probability P_s for a given contact angle $\varphi_{o,k}$ is defined as [13]

$$P_{s|\varphi_{o,k}} = P_{SNR|\varphi_{o,k}}P_{SIR|\varphi_{o,k}}, \tag{11}$$

where $P_{SNR|\varphi_{o,k}}$ and $P_{SIR|\varphi_{o,k}}$ denote the connection probability and the capture probability for a given contact angle $\varphi_{o,k}$, respectively. In particular, the connection probability $P_{SNR|\varphi_{o,k}}$ is defined as the probability that the SNR of the received signal exceeds the demodulation threshold, which can be derived as

$$P_{SNR|\varphi_{o,k}} = \Pr\left\{\frac{P_tGL\left(d\left(\varphi_{o,k}\right)\right)|h_{o,k}|^2}{\sigma^2} \geq \gamma_k\right\} \overset{(a)}{\approx} 1 - \frac{1}{\Gamma(\alpha)}\gamma\left(\alpha, \frac{\sigma^2\gamma_k}{\beta P_tGL\left(d\left(\varphi_{o,k}\right)\right)}\right), \tag{12}$$

where γ_k is the SF-specific SNR demodulation threshold of class k and step (a) follows from the substitution of the CDF given in (8). Additionally, the capture probability $P_{SIR|\varphi_{o,k}}$ is defined as the probability that the SIR of the received signal exceeds the corresponding demodulation threshold, which can be expressed as

$$P_{SIR|\varphi_{o,k}} = \Pr\left\{\frac{P_tGL\left(d\left(\varphi_{o,k}\right)\right)|h_{o,k}|^2}{\kappa\sum_{i\in\Phi_k^A\setminus o}P_tGL\left(d\left(\varphi_{i,k}\right)\right)|h_{i,k}|^2} \geq \gamma_I\right\}, \tag{13}$$

where γ_I is the SIR demodulation threshold.

Herein, we denote $I_k = \kappa\sum_{i\in\Phi_k^A\setminus o}P_tGL\left(d\left(\varphi_{i,k}\right)\right)|h_{i,k}|^2$ as the aggregated inter-ED interference. For an accurate performance analysis, we need to investigate the statistical distribution of I_k. However, due to the randomness of both channel fading and spatial point process, it is challenging to obtain the accurate statistical distribution of I_k. To tackle this challenge, we approximate the impact of aggregated inter-ED interference by that of the average inter-ED interference, i.e.,

$I_k \approx \mathbb{E}[I_k] = \bar{I}_k$ [5]. As a result, the capture probability P_{SIR} can be approximated as

$$P_{SIR|\varphi_{o,k}} \approx \Pr\left\{\frac{P_t G L\left(d\left(\varphi_{o,k}\right)\right)|h_{o,k}|^2}{\bar{I}_k} \geq \gamma_I\right\}, \quad (14)$$

with

$$\begin{aligned}\bar{I}_k &= \mathbb{E}_{I_k}\left[\kappa \sum_{i\in\Phi_k^A\setminus o} P_t G L\left(d\left(\varphi_{i,k}\right)\right)|h_{i,k}|^2\right] \\ &\overset{(b)}{=} 2\pi R^2 \kappa p_k \lambda_k P_t G \int_0^{\varphi_m} L\left(d\left(\varphi\right)\right)\mathbb{E}_{|h|^2}\left[|h|^2\right]\sin\varphi \mathrm{d}\varphi \\ &\overset{(c)}{\approx} 2\pi R^2 \kappa p_k \rho_k \lambda P_t G \alpha\beta \underbrace{\int_0^{\varphi_m} L\left(d\left(\varphi\right)\right)\sin\varphi \mathrm{d}\varphi}_{\mathcal{I}}, \end{aligned} \quad (15)$$

where step (b) follows from the Campbell's theorem [14] and the fact that the i.i.d. channel fading is independent from the spatial point process, while step (c) follows from the mean value of the approximated Gamma distribution of channel fading. Moreover, the integral $\mathcal{I}$ can be calculated as

$$\begin{aligned}\mathcal{I} &= \int_0^{\varphi_m} \frac{c_0^2 \sin\varphi}{\left(R+H\right)^2 + R^2 - 2R\left(R+H\right)\cos\varphi}\mathrm{d}\varphi \\ &\overset{(d)}{=} \int_{\cos\varphi_m}^{1} \frac{c_0^2}{\left(R+H\right)^2 + R^2 - 2R\left(R+H\right)u}\mathrm{d}u \\ &\overset{(e)}{=} \int_{v_1}^{v_2} \frac{c_0^2}{2R\left(R+H\right)v}\mathrm{d}v = \frac{c_0^2}{2R\left(R+H\right)}\ln\left(\frac{v_2}{v_1}\right), \end{aligned} \quad (16)$$

where step (d) follows $u = \cos\varphi$, step (e) follows $v = \left(R+H\right)^2 + R^2 - 2R\left(R+H\right)u$ and we denote $v_1 = H^2$, $v_2 = \left(R+H\right)^2 + R^2 - 2R\left(R+H\right)\cos\varphi_m$, $c_0 = \frac{c}{4\pi f_c}$ for simplicity.

Hence, the approximate capture probability can be simplified as

$$\begin{aligned}P_{SIR|\varphi_{o,k}} &\approx \Pr\left\{\frac{P_t G L\left(d\left(\varphi_{o,k}\right)\right)|h_{o,k}|^2}{\bar{I}_k} \geq \gamma_I\right\} \\ &\overset{(f)}{\approx} 1 - \frac{1}{\Gamma\left(\alpha\right)}\gamma\left(\alpha, \frac{c_0^2\pi R\kappa p_k\rho_k\lambda\alpha\gamma_I \ln\left(\frac{v_2}{v_1}\right)}{\left(R+H\right)L\left(d\left(\varphi_{o,k}\right)\right)}\right), \end{aligned} \quad (17)$$

where step (f) leverages the approximated Gamma distribution of channel fading described in (8).

B. System-level performance analysis

Facilitated by the PDF of contact angle $\varphi_{o,k}$ given in (3), the uplink coverage probability can be formulated as

$$\begin{aligned}P_c &= \mathbb{E}_{\varphi_{o,k}}\left[P_{s|\varphi_{o,k}}\right] = \mathbb{E}_{\varphi_{o,k}}\left[P_{SNR|\varphi_{o,k}} P_{SIR|\varphi_{o,k}}\right] \\ &= \int_0^{\varphi_m} \frac{N_s}{2}\sin\varphi_{o,k}\exp\left[-\frac{N_s}{2}\left(1-\cos\varphi_{o,k}\right)\right] \\ &\quad\times\left[1 - \frac{1}{\Gamma\left(\alpha\right)}\gamma\left(\alpha, \frac{c_0^2\pi R\kappa p_k\rho_k\lambda\alpha\gamma_I \ln\left(\frac{v_2}{v_1}\right)}{\left(R+H\right)L\left(d\left(\varphi_{o,k}\right)\right)}\right)\right] \\ &\quad\times\left[1 - \frac{1}{\Gamma\left(\alpha\right)}\gamma\left(\alpha, \frac{\sigma^2\gamma_k}{\beta P_t G L\left(d\left(\varphi_{o,k}\right)\right)}\right)\right]\mathrm{d}\varphi_{o,k}. \end{aligned} \quad (18)$$

Corollary 1. *The uplink coverage probability P_c is a monotonically decreasing function of the EDs' density λ.*

Proof: Note that P_c for a given contact angle $\varphi_{o,k}$ can be expressed as $Z \times \left[1 - \frac{1}{\Gamma(\alpha)}\gamma\left(\alpha, \frac{c_0^2\pi R\kappa p_k\rho_k\lambda\alpha\gamma_I \ln\left(\frac{v_2}{v_1}\right)}{(R+H)L(d(\varphi_{o,k}))}\right)\right]$, where

$$\begin{aligned}Z &= \frac{N_s}{2}\sin\varphi_{o,k}\exp\left[-\frac{N_s}{2}\left(1-\cos\varphi_{o,k}\right)\right] \\ &\quad\times\left[1 - \frac{1}{\Gamma\left(\alpha\right)}\gamma\left(\alpha, \frac{\sigma^2\gamma_k}{\beta P_t G L\left(d\left(\varphi_{o,k}\right)\right)}\right)\right], \end{aligned} \quad (19)$$

is independent of the EDs' density λ. Since the lower incomplete gamma function $\gamma\left(\alpha, \frac{c_0^2\pi R\kappa p_k\rho_k\lambda\alpha\gamma_I \ln\left(\frac{v_2}{v_1}\right)}{(R+H)L(d(\varphi_{o,k}))}\right)$ is increasing with respect to its second argument, P_c is a monotonically decreasing function of the EDs' density λ. The proof is completed. ∎

Furthermore, the area spectral efficiency η_k measures the information rate per unit area, which characterizes the network capacity of LoRa-based LEO satellite constellations and can be expressed as [7]

$$\eta_k = p_k\rho_k\lambda B\log_2\left(1+\gamma_k\right)P_c, \quad (20)$$

where P_c is given by (17).

Corollary 2. *The area spectral efficiency η_k is a unimodal function of the EDs' density λ.*

Proof: We first notice that $\alpha \triangleq \frac{m(2b_0+\Omega)^2}{4mb_0^2+4mb_0\Omega+\Omega^2} = \frac{4mb_0^2+4mb_0\Omega+m\Omega^2}{4mb_0^2+4mb_0\Omega+\Omega^2} > 1$ for $m > 1$. Hence, the lower incomplete gamma function $\gamma\left(\alpha, \frac{c_0^2\pi R\kappa p_k\rho_k\lambda\alpha\gamma_I \ln\left(\frac{v_2}{v_1}\right)}{(R+H)L(d(\varphi_{o,k}))}\right)$ is convex with respect to its second argument in this case, and thus P_c for a given contact angle $\varphi_{o,k}$ is concave decreasing with λ according to Corollary 1. Therefore, since η_k is the product of P_c and a positive linear function of λ, i.e., $p_k\rho_k\lambda B\log_2\left(1+\gamma_k\right)$, the area spectral efficiency is a unimodal function of the EDs' density [15]. The proof is completed. ∎

IV. Numerical Results and Discussion

In this section, we validate our proposed analytical framework through Monte-Carlo simulations. The simulation setup is illustrated as follows. Without loss of generality, we set $N_s = 1000$, $R = 6371$ km, $H = 500$ km, $L = 50$ bytes, $T_p = 3600$ s, $f_c = 868$ MHz, $B = 125$ kHz, $P_t = 16$ dBm, $N_F = 6$ dB, $G = 22.6$ dBi, and $\kappa = 10^{-3}$. Moreover, we assume that $N_p = 8$, $C = 1$, $E = 0$, and $C_r = 1$ as in [7]. The SR fading parameters are set as $m = 5.21$, $b_0 = 0.251$, and $\Omega = 0.278$, which is in accordance with [10]. In addition, the SF-specific SNR demodulation threshold γ_k is $-6, -9, -12, -15, -17.5, -20$ dB for k from 7 to 12, respectively, and the SIR demodulation threshold γ_I is set to be 6 dB [13].

Herein, Figs. 2(a) and 2(b) demonstrate the uplink coverage probability and area spectral efficiency of LoRa-based LEO satellite constellations versus the EDs' density, respectively. First, it can be observed that the numerical results of both

TABLE I
RMSE VALUES BETWEEN ANALYTICAL AND NUMERICAL RESULTS

SF	7	8	9	10	11	12
P_c	0.0211	0.0109	0.0059	0.0028	0.0019	0.0010
η_k	2.135×10^{-8}	4.788×10^{-9}	1.493×10^{-9}	4.205×10^{-10}	2.777×10^{-10}	1.645×10^{-10}

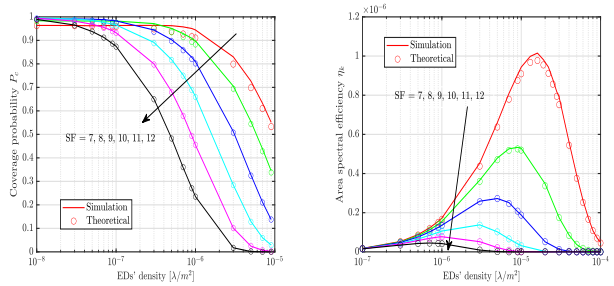

(a) Uplink coverage probability (b) Area spectral efficiency

Fig. 2. System-level performance of LoRa-based LEO satellite constellations versus the EDs' density $[\lambda/m^2]$ for (a) uplink coverage probability and (b) area spectral efficiency.

performance metrics match well with their theoretical results, which substantiates our proposed analytical framework. Moreover, Table I presents the root mean squared error (RMSE) values between the analytical and numerical results of the uplink coverage probability P_c and area spectral efficiency η_k. It can be observed that the RMSE values are very small for all SFs and become smaller with the increase of SF. Hence, the effectiveness of approximation in (14) is verified, which validates that our performance analysis remains tight in practice. Second, as illustrated in Fig. 2(a), P_c is a monotonically decreasing function of the EDs' density and better scalability performance can be achieved for smaller SFs because larger SFs could be more prone to the aggregated inter-ED interference due to the longer ToA given by (1). Third, η_k is a unimodal function of the EDs' density, as shown in Fig. 2(b), where the optimal value of λ under specific parameter settings can be obtained through the search methods. In addition, it can be seen that the maximum η_k increases dramatically for smaller SFs due to their better scalability performance. Furthermore, it can be observed that a higher P_c could be achieved for smaller EDs' density, i.e., $\lambda \leq 10^{-7}$, while higher η_k could be obtained for relatively larger EDs' density, i.e., $\lambda \geq 10^{-6}$. Hence, by tuning the EDs' density, a trade-off occurs between the scalability and network capacity of LoRa-based LEO satellite constellations.

V. CONCLUSION

In this letter, a novel analytical framework for characterizing the system-level performance of LoRa-based LEO satellite constellations was formulated. Both the channel characteristics of satellite communications and the unique features of LoRa networks were incorporated into the proposed system model to derive tractable analytical expressions for the uplink coverage probability and area spectral efficiency. Numerical simulations were conducted to verify the accuracy of our proposed analytical framework and also provide some insightful guidelines for the practical design and implementation of LoRa-based LEO satellite constellations. Overall, we believe that our work will set a solid foundation for further investigations of LoRa-based non-terrestrial networks (NTNs) in the future.

REFERENCES

[1] J. P. Shanmuga Sundaram, W. Du, and Z. Zhao, "A survey on LoRa networking: Research problems, current solutions, and open issues," *IEEE Commun. Surveys Tuts.*, vol. 22, no. 1, pp. 371-388, 1st Quart., 2020.

[2] N. Saeed, A. Elzanaty, H. Almorad, H. Dahrouj, T. Y. Al-Naffouri, and M. -S. Alouini, "CubeSat communications: Recent advances and future challenges," *IEEE Commun. Surveys Tuts.*, vol. 22, no. 3, pp. 1839-1862, 3rd Quart., 2020.

[3] M. Centenaro, C. E. Costa, F. Granelli, C. Sacchi, and L. Vangelista, "A survey on technologies, standards and open challenges in satellite IoT," *IEEE Commun. Surveys Tuts.*, vol. 23, no. 3, pp. 1693-1720, 3rd Quart., 2021.

[4] Q. Yu, D. Mishra, H. Wang, D. He, J. Yuan, and M. Matthaiou, "Closed-form access probability analysis for LoRa-based LEO satellite IoT," in *Proc. IEEE ICC*, Jun. 2025.

[5] C. C. Chan, B. Al Homssi, and A. Al-Hourani, "A stochastic geometry approach for analyzing uplink performance for IoT-over-satellite," in *Proc. IEEE ICC*, May 2022, pp. 1-6.

[6] A. Talgat, M. A. Kishk, and M. -S. Alouini, "Stochastic geometry-based uplink performance analysis of IoT over LEO satellite communication," *IEEE Trans. Aerosp. Electron. Syst.*, vol. 60, no. 4, pp. 4198-4213, Aug. 2024.

[7] L. -T. Tu, A. Bradai, Y. Pousset, and A. I. Aravanis, "On the spectral efficiency of LoRa networks: Performance analysis, trends and optimal points of operation," *IEEE Trans. Commun.*, vol. 70, no. 4, pp. 2788-2804, Apr. 2022.

[8] A. Al-Hourani, "An analytic approach for modeling the coverage performance of dense satellite networks," *IEEE Wireless Commun. Lett.*, vol. 10, no. 4, pp. 897-901, Apr. 2021.

[9] H. Jia, Z. Ni, C. Jiang, L. Kuang, and J. Lu, "Uplink interference and performance analysis for megasatellite constellation," *IEEE Internet Things J.*, vol. 9, no. 6, pp. 4318-4329, Mar. 2022.

[10] H. Jia, C. Jiang, L. Kuang, and J. Lu, "An analytic approach for modeling uplink performance of mega constellations," *IEEE Trans. Veh. Technol.*, vol. 72, no. 2, pp. 2258-2268, Feb. 2023.

[11] D. Croce, M. Gucciardo, S. Mangione, G. Santaromita, and I. Tinnirello, "Impact of LoRa imperfect orthogonality: Analysis of link-level performance," *IEEE Commun. Lett.*, vol. 22, no. 4, pp. 796-799, Apr. 2018.

[12] A. M. Zadorozhny *et al.*, "First flight-testing of LoRa modulation in satellite radio communications in low-Earth orbit," *IEEE Access*, vol. 10, pp. 100006-100023, Sep. 2022.

[13] O. Georgiou and U. Raza, "Low power wide area network analysis: Can LoRa scale?," *IEEE Wireless Commun. Lett.*, vol. 6, no. 2, pp. 162-165, Apr. 2017.

[14] M. Haenggi, *Stochastic Geometry for Wireless Networks*. Cambridge, U.K.: Cambridge Univ. Press, 2012.

[15] M. Avriel, W. E. Diewert, S. Schaible, and I. Zang, *Generalized Concavity*. Philadelphia, PA, USA: SIAM, 2010.